

Structural Characterization of Four Members of the Electron-Transfer Series $[\text{Pd}^{\text{II}}(\text{L})_2]_n$ ($\text{L} = o$ -Iminophenolate Derivative; $n = 2-, 1-, 0, 1+, 2+$). Ligand Mixed Valency in the Monocation and Monoanion with $S = 1/2$ Ground States

Swarnalatha Kokatam, Thomas Weyhermüller, Eberhard Bothe, Phalguni Chaudhuri, and Karl Wieghardt*

Max-Planck-Institut für Bioanorganische Chemie, Stiftstrasse 34-36, D-45470 Mülheim an der Ruhr, Germany

Received December 6, 2004

The reaction of the ligand 2-(2-trifluoromethyl)anilino-4,6-di-*tert*-butylphenol, $\text{H}_2(\text{L}^{\text{IP}})$, and PdCl_2 (2:1) in the presence of air and excess NEt_3 in CH_2Cl_2 produced blue-green crystals of diamagnetic $[\text{Pd}^{\text{II}}(\text{L}^{\text{ISQ}})_2]$ (**1**), where $(\text{L}^{\text{ISQ}})^{\bullet-}$ represents the *o*-iminobenzosemiquinonate(1-) π radical anion of the aromatic $(\text{L}^{\text{IP}})^{2-}$ dianion. The diamagnetic complex **1** was chemically oxidized with 1 equiv of $\text{Ag}(\text{BF}_4)$, affording red-brown crystals of paramagnetic ($S = 1/2$) $[\text{Pd}^{\text{II}}(\text{L}^{\text{ISQ}})(\text{L}^{\text{IBQ}})(\text{BF}_4)]$ (**2**), and one-electron reduction with cobaltocene yielded paramagnetic ($S = 1/2$) green crystals of $[\text{Cp}_2\text{Co}][\text{Pd}^{\text{II}}(\text{L}^{\text{ISQ}})(\text{L}^{\text{IP}})]$ (**3**); $(\text{L}^{\text{IBQ}})^0$ represents the neutral, diamagnetic quinone form. Complex **1** was oxidized with 2 equiv of $[\text{NO}]\text{BF}_4$, affording green crystals of diamagnetic $[\text{Pd}^{\text{II}}(\text{L}^{\text{IBQ}})_3(\text{BF}_4)_4\{(\text{BF}_4)_2\text{H}\}_2 \cdot 4\text{CH}_2\text{Cl}_2]$ (**5**). Oxidation of $[\text{Ni}^{\text{II}}(\text{L}^{\text{ISQ}})_2]$ ($S = 0$) in CH_2Cl_2 solution with 2 equiv of $\text{Ag}(\text{ClO}_4)$ generated crystals of $[\text{Ni}^{\text{II}}(\text{L}^{\text{IBQ}})_2(\text{ClO}_4)_2] \cdot 2\text{CH}_2\text{Cl}_2$ (**6**) with an $S = 1$ ground state. Complexes **1–5** constitute a five-membered complete electron-transfer series, $[\text{Pd}(\text{L})_2]_n$ ($n = 2-, 1-, 0, 1+, 2+$), where only species **4**, namely, diamagnetic $[\text{Pd}^{\text{II}}(\text{L}^{\text{IP}})_2]^{2-}$, has not been isolated; they are interrelated by four reversible one-electron-transfer waves in the cyclic voltammogram. Complexes **1**, **2**, **3**, **5**, and **6** have been characterized by X-ray crystallography at 100 K, which establishes that the redox processes are ligand centered. Species **2** and **3** exhibit ligand mixed valency: $[\text{Pd}^{\text{II}}(\text{L}^{\text{ISQ}})(\text{L}^{\text{IBQ}})]^+$ has localized $(\text{L}^{\text{IBQ}})^0$ and $(\text{L}^{\text{ISQ}})^{\bullet-}$ ligands in the solid state, whereas in $[\text{Pd}^{\text{II}}(\text{L}^{\text{ISQ}})(\text{L}^{\text{IP}})]^-$ the excess electron is delocalized over both ligands in the solid-state structure of **3**. Electronic and electron spin resonance spectra are reported, and the electronic structures of all members of this electron-transfer series are established.

Introduction

Square planar complexes of the type $[\text{M}^{\text{II}}(\text{L})_2]_n$, where L represents a redox-noninnocent derivative of *o*-phenylenediamide,^{1–3} $(\text{C}_6\text{H}_4(\text{NH})_2)^{2-, 1-, 0}$, or of *o*-iminophenolate, $(\text{C}_6\text{H}_4\text{O}(\text{NH}))^{2-, 1-, 0}$, and M^{II} is a divalent metal ion with a d^8 electron configuration as in Ni^{II} , Pd^{II} , and Pt^{II} ,^{4,5} are known

to form a complete five-membered electron-transfer series with $n = 2-, 1-, 0, 1+,$ and $2+$. In this work we designate the oxidation level of the ligands as is depicted in Chart 1: the aromatic, closed-shell, dianionic forms are abbreviated as $(\text{L}^{\text{IP}})^{2-}$; their monoanionic, open-shell radical forms are $(\text{L}^{\text{ISQ}})^{\bullet-}$, and the closed-shell neutral forms are $(\text{L}^{\text{IBQ}})^0$.

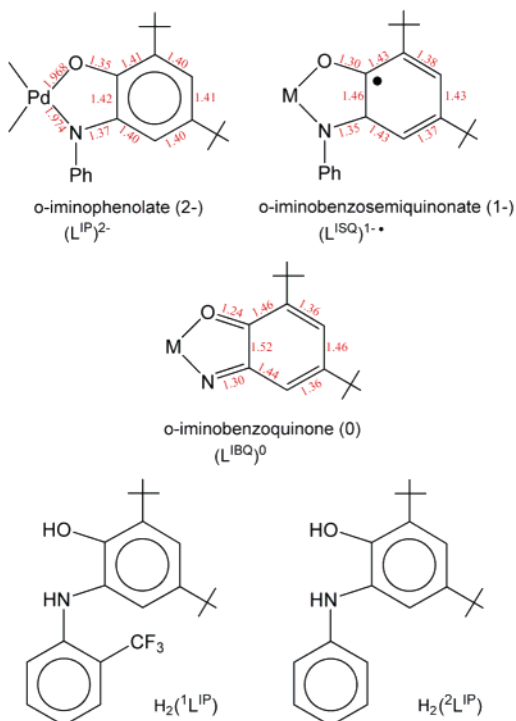
It has recently been established by density functional theoretical (DFT) and ab initio calculations that the electronic structure of the neutral complexes $[\text{M}(\text{L}^{\text{ISQ}})_2]$ is that of a singlet diradical where two $(\text{L}^{\text{ISQ}})^{\bullet-}$ π radicals are coordinated to a diamagnetic divalent central metal ion.^{3,6} The spins of

* Author to whom correspondence should be addressed. E-mail: wieghardt@mpi-muelheim.mpg.de. Phone: ++49-(0)208-306-3610. Fax: ++49-(0)208-306-3952.

(1) Balch, A. L.; Holm, R. H. *J. Am. Chem. Soc.* **1966**, *88*, 5201.
 (2) Herebian, D.; Bothe, E.; Neese, F.; Weyhermüller, T.; Wieghardt, K. *J. Am. Chem. Soc.* **2003**, *125*, 9116.
 (3) Herebian, D.; Wieghardt, K.; Neese, F. *J. Am. Chem. Soc.* **2003**, *125*, 10997.
 (4) Chaudhuri, P.; Verani, C. N.; Bill, E.; Bothe, E.; Weyhermüller, T.; Wieghardt, K. *J. Am. Chem. Soc.* **2001**, *123*, 2213.

(5) Sun, X.; Chun, H.; Hildenbrand, K.; Bothe, E.; Weyhermüller, T.; Neese, F.; Wieghardt, K. *Inorg. Chem.* **2002**, *41*, 4295.
 (6) Bachler, V.; Olbrich, G.; Neese, F.; Wieghardt, K. *Inorg. Chem.* **2002**, *41*, 4179.

Chart 1. Ligands and Oxidation Levels



the two *o*-semiquinonate(1[−]) π radicals are strongly anti-ferromagnetically coupled.

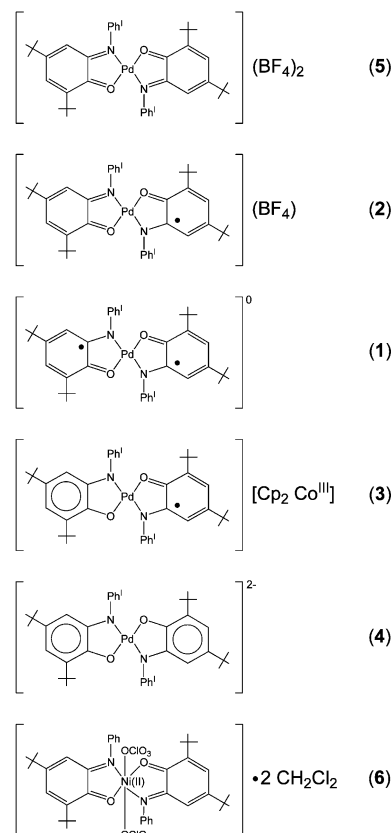
The diamagnetic dianions $[M(L^{IP})_2]^{2-}$ have been described^{1,2} as species containing a divalent d^8 metal ion ($S = 0$ in a square planar environment) and two bidentate aromatic (closed-shell) dianions $(L^{IP})^{2-}$. The crystal structure of diamagnetic $[Pd^{II}(bpy)(^2L^{IP})]^0$ has recently been reported,⁷ which confirms the presence of a single $(^2L^{IP})^{2-}$ ligand and its aromatic character therein and a neutral 2,2'-bipyridine ligand.

Similarly, although structural evidence is lacking, the diamagnetic dications have been proposed^{1–3} to contain square planar $[M^{II}(L^{IBQ})_2]^{2+}$ ions with two closed-shell quinone-type ligands and a diamagnetic central metal ion.

The most intriguing and electronically interesting species are the paramagnetic monoanions and monocations of the series, which both possess an $S_t = 1/2$ ground state. It has been proposed^{2,3,5} that the former is best described as $[M^{II}(L^{ISQ})(L^{IP})]^-$ and the latter is $[M^{II}(L^{ISQ})(L^{IBQ})]^+$. Thus, in a formal sense we are dealing with a case of mixed valency of the two ligands, which, in principle, can comprise a localized or delocalized excess electron.

To the best of our knowledge no mononuclear square planar monocationic form of this class of complexes has been structurally characterized to date. This is due to their tendency to form diamagnetic dimers with a weak $Ni\cdots Ni$ or $Pt\cdots Pt$ bond at ~ 3.0 Å.² Some of these have recently been structurally characterized, and it was found that the four ligands in such a dimer are within experimental error identical, which is indicative of a delocalized electronic

Chart 2. Complexes



structure.² The metrical details, i.e., the C–C and C–N bond lengths, were found to be intermediate between an $(L^{ISQ})^-$ and an $(L^{IBQ})^0$ ligand.

Here we report the synthesis of four members of such an electron-transfer series as solid materials and report the crystal structures of these, namely, of **1**, **2**, **3**, and **5**. These are shown in Chart 2. We have also obtained the neutral complex $[Ni^{II}(^1L^{IBQ})_2](ClO_4)_2 \cdot 2CH_2Cl_2$ (**6**), the structure of which is also reported here. This complex is similar to $[Ni^{II}(\text{tren})(^2L^{IBQ})](PF_6)_2$,⁸ which also contains a single quinone ligand, $^1L^{IBQ}$.

Experimental Section

The ligand 2-(2-trifluoromethyl)anilino-4,6-di-*tert*-butylphenol, $H_2(^1L^{IP})$, has been prepared as described previously.⁹

[Pd^{II}(¹L^{ISQ})₂] (1). A solution of the ligand $H_2(^1L^{IP})$ (1.46 g, 4.0 mmol), triethylamine (0.8 mL), and anhydrous $PdCl_2$ (0.35 g, 2.0 mmol) in acetonitrile (25 mL) was stirred under an Ar blanketing atmosphere with heating to reflux for 1 h. After this time the solution was cooled to 20 °C and stirred for 2 h in the presence of air. A blue-green precipitate formed within 12 h which was collected by filtration and recrystallized from a diethyl ether/methanol mixture (1:1 v/v), yielding blue crystals of X-ray quality. Yield: 0.45 g (30%). EI-MS: $m/z = 832$ $\{M - H\}^+$ (100). Anal. Calcd for $(C_{21}H_{24}NOF_3)_2Pd$: C, 60.57; H, 5.81; N, 3.37; Pd, 12.8. Found: C, 60.4; H, 5.8; N, 3.4; Pd, 12.9. ¹H NMR (CD_2Cl_2 , 400 MHz,

(8) Min, K. S.; Weyhermüller, T.; Wieghardt, K. *Dalton Trans.* **2003**, 1126.

(9) Bill, E.; Bothe, E.; Chaudhuri, P.; Chlopek, K.; Herebian, D.; Kokatam, S.; Ray, K.; Weyhermüller, T.; Neese, F.; Wieghardt, K. *Chem.—Eur. J.* **2005**, 204.

(7) Ghosh, P.; Begum, A.; Herebian, D.; Bothe, E.; Hildenbrand, K.; Weyhermüller, T.; Wieghardt, K. *Angew. Chem., Int. Ed.* **2003**, 42, 563.

Table 1. Crystallographic Data for **1**, **2**, **3**, **5**·0.67HBF₄·1.33CH₂Cl₂, and **6**·2CH₂Cl₂

	1	2	3	5 ·0.67HBF ₄ ·1.33CH ₂ Cl ₂	6 ·2CH ₂ Cl ₂
empirical formula	C ₄₂ H ₄₈ F ₆ N ₂ O ₂ Pd	C ₄₂ H ₄₈ BF ₁₀ N ₂ O ₂ Pd	C ₅₂ H ₅₈ CoF ₆ N ₂ O ₂ Pd	C _{43.33} H _{51.33} B _{2.67} Cl _{2.67} F _{16.67} N ₂ O ₂ Pd	C ₄₄ H ₅₂ Cl ₆ F ₆ N ₂ NiO ₁₀
fw	833.22	920.03	1022.33	1178.62	1154.29
space group	<i>P</i> 2(1)/ <i>n</i> , No. 14	<i>C</i> 2/ <i>c</i> , No. 15	<i>P</i> 1, No. 1	<i>P</i> 1̄, No. 2	<i>P</i> 2(1)/ <i>n</i> , No. 14
<i>a</i> , Å	11.1042(3)	21.5769(6)	10.1173(6)	13.5833(5)	12.8217(3)
<i>b</i> , Å	8.1767(3)	13.2251(3)	10.4874(6)	16.8101(7)	15.1119(3)
<i>c</i> , Å	21.8740(5)	30.9126(8)	12.6206(6)	18.3743(7)	13.2926(3)
α, deg	90	90	67.012(5)	78.548(5)	90
β, deg	91.81(1)	95.586(5)	73.738(5)	72.946(5)	98.210(5)
γ, deg	90	90	88.769(5)	78.209(5)	90
<i>V</i> , Å ³	1985.1(2)	8779.2(4)	1177.6(1)	3883.1(3)	2549.2(1)
<i>Z</i>	2	8	1	3	2
<i>T</i> , K	100(2)	100(2)	100(2)	100(2)	100(2)
ρ _{calcd} , g cm ⁻³	1.394	1.392	1.442	1.512	1.504
no. of reflns collected/2θ _{max}	11753/137.9	76289/56.6	31169/62.0	54535/55.0	48195/62.0
no. of unique reflns/ <i>I</i> > 2σ(<i>I</i>)	3436/3322	10873/8927	14161/13937	17684/15319	8089/6451
no. of params/restraints	242/0	535/0	604/147	1012/415	335/0
μ, cm ⁻¹ /λ, Å	43.27/1.54178	5.01/0.71073	8.00/0.71073	5.93/0.71073	7.73/0.71073
R ¹ /GOF ^b	0.0464/1.151	0.0482/1.140	0.0300/1.024	0.0568/1.128	0.0423/1.029
wR2 ^c (<i>I</i> > 2σ(<i>I</i>))	0.1352	0.0819	0.0736	0.1331	0.0984
residual density, e Å ⁻³	+1.75/−0.65	+0.81/−0.74	+1.79/−0.68	+1.18/−1.28	+0.81/−1.02

^a Observation criterion: *I* > 2σ(*I*). R1 = Σ||*F*_o − |*F*_c||/Σ|*F*_o|. ^b GOF = [Σ[w(*F*_o² − *F*_c²)]/(*n* − *p*)]^{1/2}. ^c wR2 = [Σ[w(*F*_o² − *F*_c²)]/Σ[w(*F*_o²)]]^{1/2}, where *w* = 1/σ²(*F*_o²) + (*aP*)² + *bP* [*P* = (*F*_o² + 2*F*_c²)/3].

300 K): δ = 1.01 (s, 18H); 1.08 (s, 18H); 6.03 (s, 2H); 6.63 (br, 2H); 7.48 (t, 4H); 7.65 (t, 2H); 7.77 (d, 2H).

[Pd^{II}(¹L^{1BQ})(¹L^{1SQ})](BF₄) (2**).** To a solution of **1** (0.09 g, 0.11 mmol) in CH₂Cl₂ (15 mL) was added Ag(BF₄) (21 mg; 0.11 mmol) under an Ar blanketing atmosphere. The mixture was stirred at 20 °C for 2 h and then filtered (removal of metallic Ag). Then the solvent was removed by rotary evaporation under reduced pressure, and the red-brown solid obtained was recrystallized from a CH₂Cl₂/*n*-hexane mixture (1:3). Yield: 0.07 g (70%). ESI-MS (CH₂Cl₂ solution): positive ion mode, *m/z* = 832.2 {M}+ (100); negative ion mode, *m/z* = 87.3 (100) BF₄[−]. Anal. Calcd for [(C₂₁H₂₄NOF₃)₂-Pd]BF₄: C, 54.84; H, 5.22; N, 3.04; Pd, 11.53. Found: C, 54.7; H, 5.0; N, 2.9; Pd, 11.3.

[Cp₂Co][Pd^{II}(¹L^{1SQ})(¹L^{1P})] (3**).** To a deaerated solution of **1** (0.16 g, 0.19 mmol) in CH₂Cl₂ (15 mL) was added cobaltocene, [Cp₂-Co] (36 mg, 0.19 mmol), under an Ar blanketing atmosphere. After the solution was stirred for 1 h at 10 °C, a green precipitate was obtained which was collected by filtration and recrystallized from a CH₃CN/diethyl ether mixture (1:3 v/v). Yield: 0.12 g (61%). ESI-MS (CH₂Cl₂ solution): positive ion mode, *m/z* = 188.9 (100) {Cp₂Co}⁺; negative ion mode, *m/z* = 832.5 (100) {M}[−]. Anal. Calcd for [Co(C₅H₅)₂][Pd(C₂₁H₂₄NOF₃)₂]: C, 61.16; H, 5.72; N, 2.74; Pd, 10.38. Found: C, 61.1; H, 5.6; N, 2.8; Pd, 10.3.

[Pd^{II}(¹L^{1BQ})₂]₃(BF₄)₄{(BF₄)₂H}₂·4CH₂Cl₂ (5**).** To a deaerated solution of **1** (0.075 g, 0.09 mmol) in CH₂Cl₂ (15 mL) was added [NO]BF₄ (23 mg, 0.19 mmol) under an Ar blanketing atmosphere. It is noted that the crude, commercially available (Aldrich) [NO]-BF₄ was used, which is contaminated with HF. The solution was stirred at 20 °C for 3 h. The reaction volume was reduced to half by slow evaporation of the solvent, and *n*-hexane (15 mL) was added. The solution was allowed to stand at −10 °C for 12 h. The green precipitate was filtered off and recrystallized from a CH₂Cl₂/*n*-hexane mixture (1:3 v/v). Yield: 0.06 g (~60%). Anal. Calcd for [Pd(C₂₁H₂₄NOF₃)₂]₃(BF₄)₄{(BF₄)₂H}₂·4CH₂Cl₂: C, 46.48; H, 4.56; N, 2.50; Pd, 9.47. Found: C, 46.9; H, 4.7; N, 2.5; Pd, 9.56.

[Ni^{II}(¹L^{1BQ})₂(ClO₄)₂]·2CH₂Cl₂ (6**).** To a deaerated solution of [Ni(¹L^{1SQ})₂] (0.25 g, 0.32 mmol) in CH₂Cl₂ (30 mL) was added solid AgClO₄·H₂O (0.13 g, 0.64 mmol) under an Ar blanketing atmosphere. The mixture was stirred at 20 °C for 2 h and was then filtered (removal of Ag⁰). After removal of the solvent by rotary evaporation under reduced pressure the red-orange residue was

recrystallized from a CH₂Cl₂/*n*-hexane mixture (1:2 v/v). Yield: 0.12 g (40%). ESI-MS: positive ion mode, *m/z* = 883.3 (100) {M − ClO₄}⁺. Anal. Calcd for Ni(C₂₁H₂₄NOF₃)₂(ClO₄)₂·2CH₂Cl₂: C, 45.87; H, 4.55; N, 2.43; Ni, 5.09. Found: C, 46.1; H, 4.7; N, 2.3; Ni, 4.9.

X-ray Crystallographic Data Collection and Refinement of the Structures. Dark green single crystals of **3** and **5** and deep red crystals of **2** and **6** were coated with perfluoropolyether and immediately mounted in the nitrogen cold stream (100 K) of a Nonius Kappa-CCD diffractometer equipped with a Mo target rotating-anode X-ray source and a graphite monochromator (Mo Kα, λ = 0.71073 Å). A dark red crystal of **1** was measured on a Bruker SMART diffractometer, equipped with a copper rotating anode at 100 K (Cu Kα, λ = 1.54178 Å). Final cell constants were obtained from least-squares fits of all measured reflections. Crystal faces of **3**, **5**, and **6** were determined, and the corresponding intensity data were corrected for absorption using the Gaussian-type routine embedded in XPREP.¹⁰ Data set **1** was corrected using the program SADABS.¹¹ Crystallographic data of the compounds are listed in Table 1. The Siemens ShelXTL¹⁰ software package was used for solution and artwork of the structure; ShelXL97¹² was used for the refinement. The structures were readily solved by direct and Patterson methods and subsequent difference Fourier techniques. All non-hydrogen atoms were refined anisotropically. Hydrogen atoms attached to carbon atoms were placed at calculated positions and refined as riding atoms with isotropic displacement parameters.

In a first attempt, complex **3** was refined in centrosymmetric space group *P*1̄ (No. 2), but this refinement suffered from disorder of (trifluoromethyl)phenyl groups (PhCF₃) of the anion and severe disorder of the cobaltocenium cation, each of them residing on a center of inversion. A closer inspection of the structure revealed that the disorder of the cation disappears upon refinement in the chiral space group *P*1 (No. 1). Refinement of the disordered PhCF₃ groups of the anion clearly showed that the occupation factors for both PhCF₃ units were different on either side of the *pseudoinversion* center (52:48 vs 87:13). The geometry of the phenyl rings was fixed using AFIX 66; the CF₃ group, N—C^{phenyl} distances, and

(10) ShelXTL V.5, Siemens Analytical X-Ray Instruments, Inc., Madison, WI, 1994.

(11) SADABS 2004, Bruker Nonius, Delft, The Netherlands, 2004.

(12) Sheldrick, G. M. ShelXL97, Universität Göttingen, Germany, 1997.

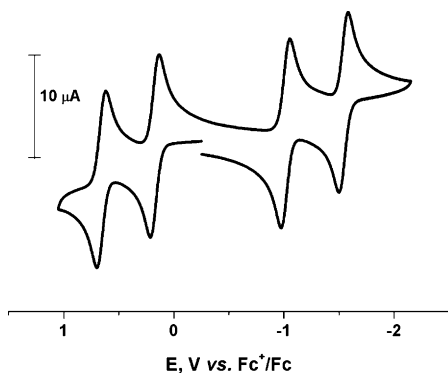


Figure 1. Cyclic voltammogram of $[\text{Pd}^{\text{II}}(\text{1L}^{\text{ISQ}})_2]$ (**1**) in CH_2Cl_2 solution containing 0.10 M $[\text{N}(n\text{-bu})_4]\text{PF}_6$ as supporting electrolyte. Conditions: 20 °C, glassy carbon working electrode, scan rate 100 mV s^{-1} , ferrocene internal standard.

thermal displacement parameters of “chemically equal” atoms of both PhCF_3 groups were restrained by SADI and EADP instructions. The structure is probably most accurately described as a racemic twin consisting of two rotamers with respect to the orientation of the CF_3 groups.

Compound **5** crystallizes in space group *P1*. The asymmetric unit consists of two crystallographically independent complex cations of the *syn*- and *anti*-rotamers, the latter lying on a center of inversion, four fully occupied “ BF_4 positions”, and two CH_2Cl_2 molecules of crystallization. Two BF_4 positions were found to be in close proximity of F(201), having short $\text{F}\cdots\text{F}$ contacts at 2.57 Å ($\text{F}(201)\cdots\text{F}(303)$) and 2.69 Å ($\text{F}(201)\cdots\text{F}(104)$). A close inspection of F(201) revealed a weak density peak at a distance of 0.9 Å which was assigned to a hydrogen. The assignment is supported by the fact that the $\text{F}-\text{H}$ vector points directly to the neighboring F(303). Therefore, the unit cell contains three complex dications, six BF_4 anions, 2 mol of HBF_4 , and four molecules of CH_2Cl_2 . The two BF_4 anions involved in the hydrogen bonding to HBF_4 were found to be disordered and were split on two positions. $\text{B}-\text{F}$ and $\text{F}-\text{F}$ distances were restrained to be equal within error (SADI). Equal thermal displacement parameters were given to the corresponding parts (EADP). A CH_2Cl_2 molecule (C(600)) was likewise split on two positions. $\text{C}-\text{Cl}$ and $\text{Cl}-\text{Cl}$ distances were restrained using SADI and EADP instructions. The coordinated ClO_4 anion of compound **6** was found to be disordered on two positions with equal occupation factors. Equal anisotropic displacement parameters were attributed to corresponding atoms.

Results

Syntheses and Characterization. When a solution of ligand $\text{H}_2(\text{1L}^{\text{IP}})$ and excess NEt_3 reacted with PdCl_2 in acetonitrile in the presence of air, a deep blue-green precipitate of the square planar, neutral complex $[\text{Pd}^{\text{II}}(\text{1L}^{\text{ISQ}})_2]$ (**1**) was obtained. The compound is diamagnetic as judged from its normal ^1H NMR spectrum (see the Experimental Section). The corresponding complex $[\text{Pd}(\text{2L}^{\text{ISQ}})_2]$ has been described previously.⁴

Figure 1 displays the cyclic voltammogram of **1** in CH_2Cl_2 solution containing 0.10 M $[\text{N}(n\text{-bu})_4]\text{PF}_6$ as supporting electrolyte and a glassy carbon working electrode. All potentials are referenced vs the ferrocenium/ferrocene couple (Fc^+/Fc). Four reversible one-electron-transfer waves are observed at $E_{1/2}$ values of +0.65, +0.17, -1.01, and -1.54 V vs Fc^+/Fc . Controlled-potential coulometric measurements

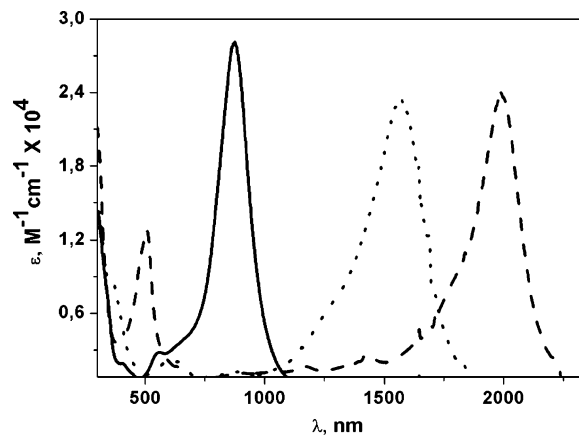


Figure 2. Electronic spectra of **1** (solid line), its electrochemically one-electron-oxidized form $[\text{Pd}(\text{1L})_2]^+$ (**2**) (dashed line), and its one-electron-reduced form $[\text{Pd}(\text{1L})_2]^{1-}$ (**3**) (dotted line) in CH_2Cl_2 solution (0.20 M $[\text{N}(n\text{-bu})_4]\text{PF}_6$) at 20 °C.

Table 2. Electronic Spectra of the Complexes in CH_2Cl_2 Solution

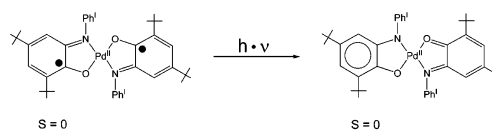
complex	λ_{max} , nm (ϵ , $\text{M}^{-1} \text{s}^{-1}$)
1	871 (2.7×10^4), 546 (0.2×10^4), 403 sh (0.2×10^4)
2	1986 (2.5×10^4), 1432 (0.23×10^4), 1173 (0.2×10^4), 875 (0.3×10^4), 507 (1.3×10^4)
3	1564 (2.4×10^4), 872 (0.13×10^4), 615 (0.21×10^4), 360 sh (0.9×10^4)
4^a	592 (0.2×10^4), 359 (1.3×10^4)
5^b	625 (0.25×10^4), 394 (1.8×10^4), 331 (1.8×10^4)
6	480 (0.5×10^4), 350 sh (0.4×10^4)

^a Refers to the electrochemically generated dianion $[\text{Pd}^{\text{II}}(\text{1L}^{\text{IP}})_2]^{2-}$.
^b Refers to the electrochemically generated dication $[\text{Pd}^{\text{II}}(\text{1L}^{\text{IBQ}})_2]^{2+}$.

established that **1** is twice one-electron-oxidized, yielding a mono- and a dication, and twice one-electron-reduced, yielding a mono- and dianion. Thus, a complete electron-transfer series consisting of five species $[\text{Pd}^{\text{II}}(\text{1L})_2]^n$ ($n = 2+, 1+, 0, 1-, 2-$) has been established as has been previously done for $[\text{Pd}(\text{2L})_2]$ with quite similar $E_{1/2}$ values of +0.47, +0.08, -0.99, and -1.40.⁴

The electronic spectrum of **1** (shown in Figure 2; see also Table 2) exhibits a very intense spin- and dipole-allowed ligand-to-ligand charge-transfer band (LLCT) at 871 nm ($\epsilon = 2.7 \times 10^4 \text{ M}^{-1} \text{ cm}^{-1}$).

This absorption band is characteristic for all square planar $[\text{M}^{\text{II}}(\text{L}^{\bullet})_2]$ complexes.¹⁻³

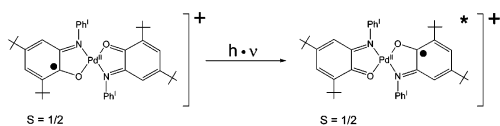


Since the coulometric measurements on CH_2Cl_2 solutions of **1** clearly showed that the reduced and oxidized forms are stable at ambient temperature for many hours, we attempted to generate these forms chemically by using silver ions or $[\text{NO}]\text{BF}_4$ as oxidant and cobaltocene as reductant. Thus, oxidation of **1** with 1 equiv of AgBF_4 in CH_2Cl_2 solution produced a red-brown solid of $[\text{Pd}^{\text{II}}(\text{1L}^{\text{ISQ}})(\text{1L}^{\text{IBQ}})](\text{BF}_4)$ (**2**). Molar magnetic susceptibility measurements in the range 4–300 K revealed a temperature-independent magnetic moment of 1.7 μ_{B} , indicating a paramagnetic $S = 1/2$ ground state for **2**. The X-band EPR spectrum of **2** in frozen CH_2Cl_2

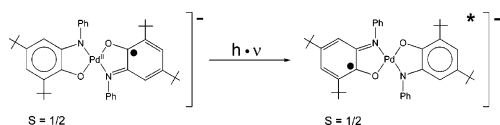
Cl_2 at 10 K displays a narrow signal at $g_{\text{iso}} = 2.0007$ (width 10 mT) which is typical for square planar monocationic species $[\text{M}(\text{L})_2]^+$ (see Table 5 in ref 2). This confirms the $S = 1/2$ ground state and indicates that the unpaired electron resides predominantly on a ligand as in $(^1\text{L}^{\text{ISQ}})^{\bullet-}$. The electronic structure of **2** is thus best described as $[\text{Pd}(^1\text{L}^{\text{ISQ}})(^1\text{L}^{\text{IBQ}})]^+$.

Figure 2 shows the electronic spectrum of **2** (see also Table 2). The spectrum is dominated by a very intense “intervalence band” at 1992 nm ($\epsilon = 2.5 \times 10^4 \text{ M}^{-1} \text{ cm}^{-1}$).

The intense absorption maximum at 504 nm ($\epsilon = 1.28 \times 10^4 \text{ M}^{-1} \text{ cm}^{-1}$) is characteristic for the presence of a *N,O*-coordinated *o*-iminobenzoquinone, $(^1\text{L}^{\text{IBQ}})^0$, ligand. For the uncoordinated organic molecule $(\text{L}^{\text{IBQ}})^0$ in CH_2Cl_2 this maximum is observed² at 488 nm (as well as a shoulder at 396 nm).



The reduction of **1** with 1 equiv of $[\text{Cp}_2\text{Co}^{\text{II}}]$ (Cp is the cyclopentadienyl anion) in CH_2Cl_2 under strictly anaerobic conditions affords a green precipitate of $[\text{Cp}_2\text{Co}^{\text{III}}][\text{Pd}^{\text{II}}(^1\text{L}^{\text{ISQ}})(^1\text{L}^{\text{IP}})]$ (**3**). Magnetic susceptibility measurements (4–300 K) revealed a temperature-independent magnetic moment of $1.7 \mu_{\text{B}}$ for **3**, indicating an $S = 1/2$ ground state. The X-band EPR spectrum of **3** in frozen CH_2Cl_2 at 10 K reveals a rhombic signal with parameters $g_1 = 2.0715$, $g_2 = 2.0167$, and $g_3 = 1.974$ ($g_{\text{iso}} = 2.021$). Similar signals have been reported for many square planar monoanions $[\text{M}(\text{L})_2]^-$ (see Table 5 in ref 2). The unpaired electron resides predominantly on the ligands.^{3,5} The electronic spectrum of **3** shown in Figure 2 shows the expected intense intervalence band(s) at 1547 nm ($2.8 \times 10^4 \text{ M}^{-1} \text{ cm}^{-1}$).



All attempts to generate a solid material containing the dianion $[\text{Pd}^{\text{II}}(^1\text{L}^{\text{IP}})_2]^{2-}$ (**4**) have failed due to the extreme oxygen sensitivity of this species. The electronic spectrum of this electrochemically generated dianion has been successfully recorded and is shown in Figure 3. A single relatively intense ligand-to-metal charge-transfer band is observed at 592 nm ($\epsilon = 0.2 \times 10^4 \text{ M}^{-1} \text{ cm}^{-1}$), and no LLCT band is observed at $>600 \text{ nm}$.

In contrast, the two-electron oxidation of **1** by 2 equiv of $[\text{NO}]\text{BF}_4$ in CH_2Cl_2 successfully generated green, diamagnetic $[\text{Pd}^{\text{II}}(^1\text{L}^{\text{IBQ}})_2](\text{BF}_4)_4 \cdot \{(\text{BF}_4)_2\text{H}\}_2 \cdot 4\text{CH}_2\text{Cl}_2$ (**5**). Its electronic spectrum exhibits two absorption maxima characteristic of $^1\text{L}^{\text{IBQ}}$ ligands at 625 and 394 nm (Figure 3, Table 2). Magnetic susceptibility measurements in the temperature range 4–300 K reveal that **5** possesses an $S = 0$ ground state. Similarly, from the reaction of $[\text{Ni}^{\text{II}}(^1\text{L}^{\text{ISQ}})_2]$ in CH_2Cl_2 ⁹ with 2 equiv of $\text{AgClO}_4 \cdot \text{H}_2\text{O}$ red-orange crystals of

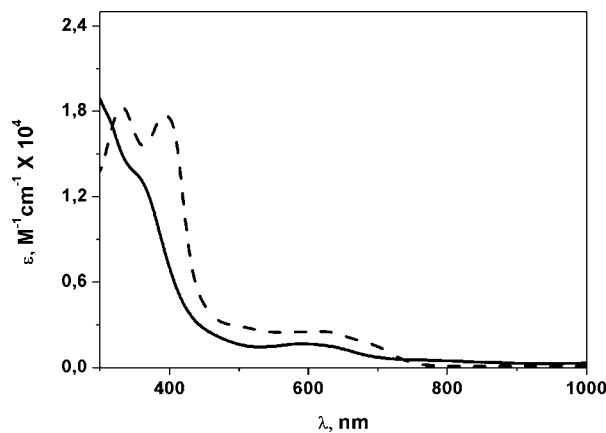


Figure 3. Electronic spectra of electrochemically generated $[\text{Pd}(^1\text{L})_2]^{2+}$ (**5**) (dashed line) and of $[\text{Pd}(^1\text{L})_2]^{2-}$ (**4**) (solid line) in CH_2Cl_2 solution (0.20 M $[\text{N}(n\text{-bu})_4]\text{PF}_6$).

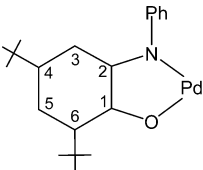
$[\text{Ni}^{\text{II}}(^1\text{L}^{\text{IBQ}})_2(\text{ClO}_4)_2] \cdot 2\text{CH}_2\text{Cl}_2$ (**6**) were obtained. Its electronic spectrum shows the presence of two $^1\text{L}^{\text{IBQ}}$ molecules (Table 2). Temperature-dependent (4–300 K) magnetic susceptibility measurements clearly indicate that **6** is paramagnetic with an $S = 1$ ground state: $\mu_{\text{eff}}(50\text{--}300 \text{ K}) = 2.88 \mu_{\text{B}}$; $g = 2.04$, $|D| = 5.5 \text{ cm}^{-1}$, $\text{TIP} = 0.25 \times 10^{-3} \text{ m}^3 \text{ mol}^{-1}$.

Crystal Structures. The crystal structures of **1**, **2**, **3**, and **5**, which represent four out of five possible members of the complete electron-transfer series $[\text{Pd}(\text{L})_2]^n$ ($n = 2-, 1-, 0, 1+, 2+$), have been determined by using data sets collected at 100 K. The structure of the nickel complex **6** has also been determined. Table 1 summarizes crystallographic data, and Table 3 gives selected bond distances.

In **1**, **2**, **3**, and **5** the palladium(II) ions are always *N,O*-coordinated to two ligands in *trans* positions relative to each other at various oxidation levels, namely, $(^1\text{L}^{\text{IP}})^{2-}$, $(^1\text{L}^{\text{ISQ}})^{\bullet-}$, or $(^1\text{L}^{\text{IBQ}})^0$, giving rise to square planar coordination polyhedra, *trans*- PdN_2O_2 . Figure 4 displays the structures of (a) the neutral species in crystals of **1** (top) and (b) the monocation in crystals of **2**.

In our previous work we had shown that the C–C, C–N, and C–O bond distances of the ligands vary significantly within their varying oxidation levels.^{4–7} Thus, the distances summarized in Chart 1 were derived from high-quality crystal structures of (1) $[(\text{bpy})\text{Pd}^{\text{II}}(^2\text{L}^{\text{IP}})]^7$ for the closed-shell dianion $(\text{L}^{\text{IP}})^{2-}$, (2) $[\text{Pd}^{\text{II}}(^2\text{L}^{\text{ISQ}})_2]^{4-}$ and $[\text{Ni}^{\text{II}}(\text{tren})(^2\text{L}^{\text{ISQ}})](\text{ClO}_4)$ for the π radical monoanion $(\text{L}^{\text{ISQ}})^{\bullet-}$,⁸ and (3) $[\text{Ni}^{\text{II}}(\text{tren})(^2\text{L}^{\text{IBQ}})](\text{PF}_6)_2$ for the closed-shell neutral quinone form (tren = tris(2-aminoethyl)amine).⁸

The following markers can be identified on going from the *N,O*-coordinated $(\text{L}^{\text{IP}})^{2-}$ dianion to the $(\text{L}^{\text{ISQ}})^{\bullet-}$ monoanionic π radical, and then to the neutral quinone $^2\text{L}^{\text{IBQ}}$: (a) The C–N bond lengths decrease from 1.37 ± 0.01 to 1.35 ± 0.01 and finally to $1.30 \pm 0.01 \text{ \AA}$ with increasing oxidation level. (b) Similarly, the C–O bond lengths decrease from 1.35 ± 0.01 to 1.30 ± 0.01 to $1.24 \pm 0.01 \text{ \AA}$. (c) Finally, the six C–C bonds of the aminophenolate six-membered ring of $(^2\text{L}^{\text{IP}})^{2-}$ are nearly equidistant at $1.407 \pm 0.01 \text{ \AA}$, indicating the aromatic character of the phenyl ring. One-electron oxidation to $(^2\text{L}^{\text{ISQ}})^{\bullet-}$ results in two alternating short C–C bonds at $1.375 \pm 0.01 \text{ \AA}$ of partially double bond

Table 3. Selected Bond Distances (Å) in the Complexes


	1	2^a		3^a		[Pd^{II}(bpy)(²L^{IBQ})]^e	5^b	6
Pd–N	1.963(2)	2.011(2)	1.966(2)	1.960(2)	1.996(2)	(1.974(2))	1.998(5)	2.049(1) ^c
Pd–O	1.975(2)	1.997(2)	1.974(2)	2.001(2)	1.984(2)	(1.968(1))	2.005(2)	2.030(1) ^d
C2–N	1.354(4)	1.316(3)	1.345(3)	1.377(3)	1.378(3)	1.387(2)	1.301(5)	1.296(2)
C1–O	1.314(4)	1.255(3)	1.313(3)	1.329(3)	1.341(3)	1.348(2)	1.252(5)	1.239(2)
C1–C2	1.437(5)	1.491(3)	1.443(3)	1.422(4)	1.426(4)	1.421(3)	1.506(6)	1.513(2)
C2–C3	1.413(4)	1.424(3)	1.417(3)	1.406(4)	1.406(3)	1.395(2)	1.430(6)	1.438(2)
C3–C4	1.377(4)	1.353(3)	1.362(3)	1.388(4)	1.391(4)	1.402(2)	1.350(6)	1.352(2)
C4–C5	1.421(4)	1.478(3)	1.445(3)	1.401(4)	1.400(4)	1.398(3)	1.472(6)	1.473(2)
C5–C6	1.377(4)	1.350(3)	1.376(3)	1.403(4)	1.396(4)	1.405(3)	1.353(6)	1.357(2)
C6–C1	1.427(4)	1.450(3)	1.427(3)	1.426(4)	1.405(4)	1.406(2)	1.447(6)	1.460(2)

^a Corresponding bond lengths are given for two crystallographically independent ligands in [Pd(L^{IBQ})(L^{ISQ})](BF₄) (**2**) and [Pd(L^{IP})(L^{ISQ})](Cp₂Co) (**3**).
^b Averaged values. ^c Ni–N. ^d Ni–O. ^e Reference 7.

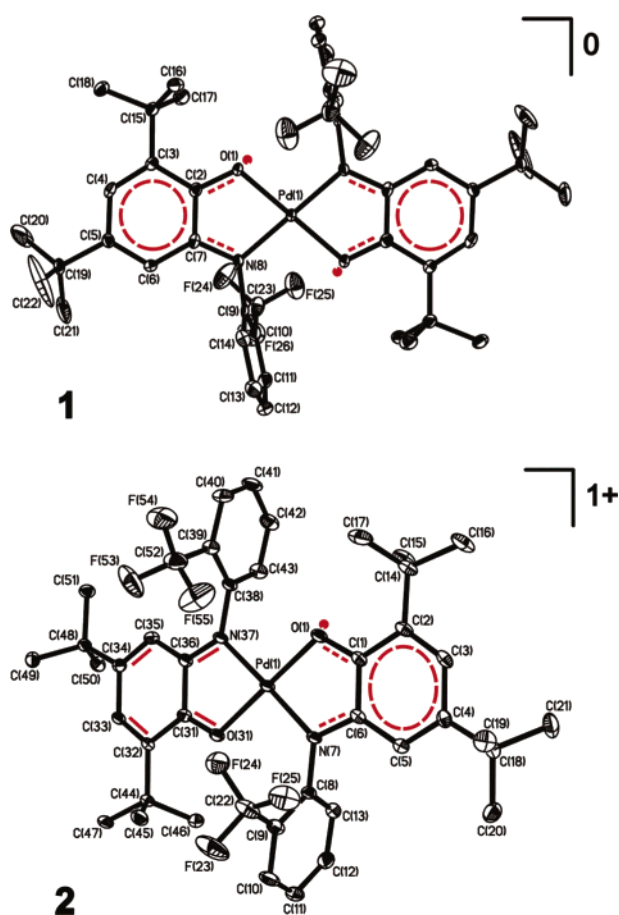


Figure 4. Structure of the neutral complex [Pd^{II}(¹L^{ISQ})₂] in crystals of **1** (top) and of the monocation [Pd^{II}(¹L^{ISQ})(¹L^{IBQ})]⁺ in crystals of **2**. The structure of the monoanion in **3** resembles that of **2** and is not shown. The structural features given in red represent our interpretation of the bonding situation in the ligands.

character and four longer ones at 1.438 ± 0.01 Å. This characteristic distortion is labeled “quinoid-like”. In the neutral genuine quinone form ²L^{IBQ}, this distortion is more pronounced with two alternating short C=C double bonds

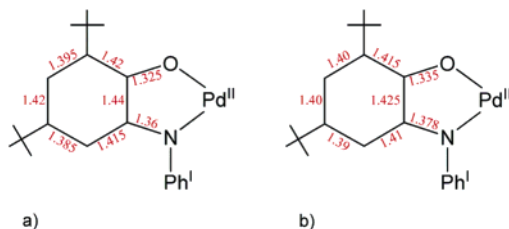
at 1.36 ± 0.01 Å and four long C–C single bonds, one of which at 1.52 ± 0.01 Å being a normal C–C single bond.

Using the above criteria for the assignment of oxidation levels of the two ligands in **1**, it is immediately clear that two crystallographically identical (¹L^{ISQ})^{•−} π radical monoanions are present, which affords an oxidation state of II for the central metal ion (d⁸, S_{Pd} = 0 in a square planar ligand field). The diamagnetic ground-state S_T = 0 is then attained via very strong intramolecular antiferromagnetic coupling between the spins of the ligand radicals. Complex **1** is a diradical with a singlet ground state.^{2,3,5,6} We also note that the two crystallographically identical (trifluoromethyl)phenyl groups in **1** in *trans* positions relative to each other are positioned in such a way that one CF₃ group is above the PdL₂ plane and the other one is below this plane (*anti*-rotamer).

The structure of **2** reveals that monocations [Pd^{II}(¹L^{ISQ})(¹L^{IBQ})]⁺ and BF₄[−] anions are present in a 1:1 ratio. Interestingly, the cation does not possess crystallographically imposed symmetry; both N,O-coordinated ligands in *trans* positions relative to each other are crystallographically independent. It is remarkable that the CF₃ groups of both ligands are located on the same side of the PdL₂ plane (*syn*-rotamer). Unexpectedly, the C–C, C–N, and C–O bond lengths of both ligands *differ* in a characteristic fashion, which allows us to assign ligand oxidation levels as (¹L^{ISQ})^{•−} for one ligand (N7, O1, C1–C6) but ¹L^{IBQ} for the other one (N37, O31, C31–C36). This ligand oxidation level distribution yields again an oxidation state of II for the central palladium ion (d⁸, S_{Pd} = 0). The unpaired electron of the S_T = 1/2 ground state is localized on the single (¹L^{ISQ})^{•−} ligand; it is not significantly delocalized over both ligands in the solid state. This localization in the solid state is due to an unsymmetrical ion pairing between the cation and the BF₄[−] anion. The latter is located above the (L^{IBQ}) plane and involves a weak F(63)⋯C(31) interaction at 2.709 Å.

It is also noteworthy that the two Pd–N bond distances at 1.966 ± 0.006 Å for the (¹L^{ISQ})^{•−} ligand and at $2.011 \pm$

Chart 3. (a) Calculated Arithmetic Mean Values of Corresponding Bond Lengths (Å) of the $Pd(^1L^{ISQ})^-$ and $Pd(^1L^{IP})$ Units Given in Chart 1 and (b) Experimental Bond Lengths (Å) of the Monoanion $[Pd^{II}(^1L^{ISQ})(^1L^{IP})]^-$ in Crystals of **3**



0.006 Å for the $^1L^{BQ}$ ligand differ significantly; the same holds true for the corresponding two Pd–O distances at 1.974 ± 0.006 and 1.997 ± 0.006 Å. It is also gratifying that the dimensions of the $Pd(^1L^{ISQ})$ part in both **1** and **2** are identical within experimental error.

The structure of **3** consists of monoanions $[Pd^{II}(^1L^{IP})(^1L^{ISQ})]^-$ and well-separated cobalticenium cations $[Cp_2Co^{III}]^+$ in the ratio 1:1. The overall structure of the monoanion is very similar to that of the monocation in **2**. Both CF_3 groups are on the same side of the PdL_2 plane; both N,O -coordinated ligands are crystallographically independent. It is now quite remarkable that the C–C, C–N, and C–O distances of both ligands in **3** are within experimental error (± 0.01 Å) identical, which is in stark contrast to the structure of the monocation in **2**. It is also noteworthy that the averaged C–C, C–N, and C–O bonds in **3** do not allow straightforward assignment of the ligand oxidation level using the data in Chart 1. Rather, it appears that these distances are close to the arithmetic mean between those of $(L^{IP})^{2-}$ and $(L^{ISQ})^-$ as shown in Chart 3. This result implies that the excess electron in $[Pd^{II}(^1L^{IP})(^1L^{ISQ})]^-$ is delocalized over both ligands.

Complex **5** crystallizes in the triclinic space group $P\bar{1}$ with three $[Pd^{II}(^1L^{BQ})_2]^{2+}$ dications and four well-separated BF_4^- anions as well as two $\{(BF_4)_2H\}^-$ monoanions and four molecules of CH_2Cl_2 of crystallization per unit cell. One Pd^{II} ion lies on a center of symmetry, whereas the other two occupy a symmetry-related general position. Interestingly, the conformations of the two crystallographically different dications are not the same (Figure 5): while in the first one both CF_3 groups are in *anti* positions relative to each other, these are located on the same side of the PdL_2 plane in the second. The C–O, C–N, and C–C and the Pd–N and Pd–O distances in both rotamers are within experimental error identical. The bond lengths within the ligands agree nicely with those given in Chart 1 for the quinone oxidation level, $^1L^{BQ}$. Thus, an electronic structure such as $[Pd^{II}(^1L^{BQ})_2]^{2+}$ is established unequivocally by X-ray crystallography. The presence of two $\{(BF_4)_2H\}^-$ monoanions is clearly established by the short $F\cdots F$ distance of ~ 2.6 Å between two BF_4^- groups. A few other examples for the presence of this anion were identified by a search in the Cambridge X-Ray Crystallographic Data Base.¹³

(13) Goodfellow, R. G.; Hamon, E. M.; Howard, J. A. K.; Spencer, J. L.; Turner, D. G. *Chem. Commun.* **1984**, 1604.

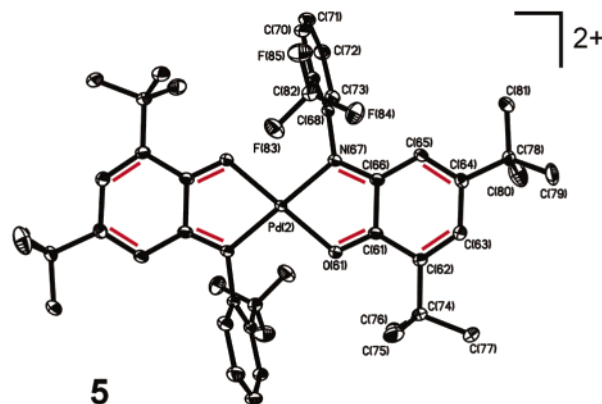
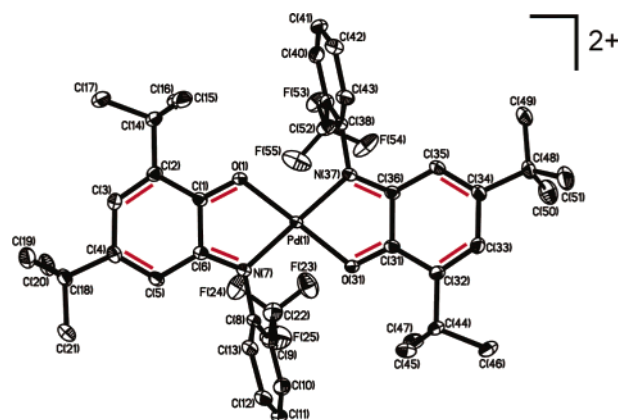


Figure 5. Structures of the two dicationic conformers in crystals of **5**. The structural features given in red represent our interpretation of the bonding situation in the ligands.

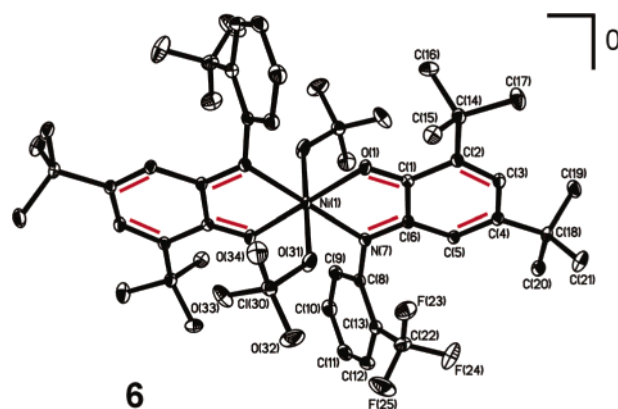


Figure 6. Structure of the neutral molecule $[Ni^{II}(^1L^{BQ})_2(OClO_3)_2]$ in crystals of **6**. The structural features given in red represent our interpretation of the bonding situation in the ligands.

Figure 6 shows the structure of the neutral molecule $[Ni^{II}(^1L^{BQ})_2(OClO_3)_2]$ in crystals of **6**. Two N,O -coordinated $^1L^{BQ}$ ligands are coordinated in an equatorial plane—in *trans* positions relative to each other. The axial positions are occupied by two oxygen atoms, each from an O -coordinated perchlorate anion. This neutral octahedral molecule has an $S = 1$ ground state as expected. The dimensions of the bound $^1L^{BQ}$ ligands are exactly those given in Chart 1 for such a quinone-like oxidation level. They are the same as those observed in the $Pd^{II}(^1L^{BQ})$ part in the monocation of **2** and in both ligands of the dications in **5**.

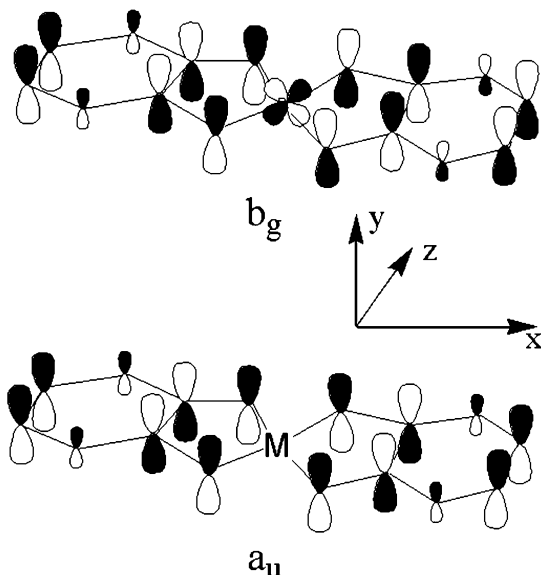


Figure 7. The two redox-active MOs of **1–5**. The a_u MO is lower in energy, whereas the b_g MO is higher in energy.

Discussion

The electronic structures of $[\text{Ni}^{\text{II}}(\text{L}_\text{N}^{\text{ISQ}})_2]$ and of $[\text{Pt}^{\text{II}}(\text{L}_\text{O}^{\text{ISQ}})_2]$, where $(\text{L}_\text{N}^{\text{ISQ}})^{\bullet-}$ represents the *o*-diiminobenzosemiquinonate(1 $-$) and $(\text{L}_\text{O}^{\text{ISQ}})^{\bullet-}$ the *o*-iminobenzosemiquinonate(1 $-$) radical anion, have been calculated by (relativistic) density functional theoretical and correlated ab initio methods.^{2,3,5,6} It has been shown that their electronic structures and that of their monocations and -anions can be understood in terms of a simple model which involves only two redox-active molecular orbitals depicted in Figure 7 which are basically the symmetric and antisymmetric combination of the SOMO of the free (uncoordinated) semiquinonate(1 $-$) ligand. In **1**, **2**, **3**, and **5** four filled metal d orbitals of lower energy indicate the presence of a diamagnetic d^8 configuration of a central nickel(II) or palladium(II) ion. We propose here that the electronic structures of $[\text{Pd}^{\text{II}}(\text{L}_\text{O}^{\text{ISQ}})_2]$ (the truncated form of **1**), as well as those of the monoanion and -cation and of the dication and -anions, can be understood analogously as shown in Figure 8.

Thus, the diamagnetic dianion $[\text{Pd}^{\text{II}}(\text{L}^{\text{IP}})_2]^{2-}$ possesses a closed-shell configuration, $(a_u)^2(b_g)^2$, with two iminophenolate(2 $-$) ligands and a central Pd^{II} ion. Similarly, the diamagnetic dication $[\text{Pd}^{\text{II}}(\text{L}^{\text{IBQ}})_2]^{2+}$ consists of two closed-shell quinone ligands and a central Pd^{II} ion. The ground-state configuration possesses an $(a_u)^0$ LUMO which is a ligand π^* orbital. The structural parameters of **5** support this interpretation.

The monoanion $[\text{Pd}^{\text{II}}(\text{L}^{\text{ISQ}})(\text{L}^{\text{IP}})]^-$ possesses an $(a_u)^2(b_g)^1$ ground state which transforms “gerade” under inversion.^{3,5} It, therefore, mixes readily with the out-of-plane d_{xz} orbital of the $\text{Pd}(\text{II})$ ion and acquires thereby some metal character. Since the above ground state mixes readily with energetically relatively low-lying d–d excited states, it has a sizable orbital angular momentum which manifests itself in the relatively large g shift observed experimentally for this monoanion.

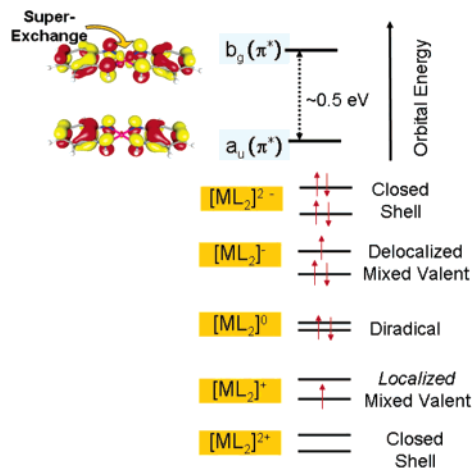


Figure 8. Summary of the electronic structures of the five members of the electron-transfer series $[\text{Pd}^{\text{II}}(\text{L})_2]^z$ ($z = 2+, 1+, 0, 1-, 2-$). The two highest energy molecular orbitals (see also Figure 7) are considered only.

In contrast, the same bonding model predicts an $(a_u)^1(b_g)^0$ ground state for the monocation $[\text{Pd}^{\text{II}}(\text{L}^{\text{ISQ}})(\text{L}^{\text{IBQ}})]^+$ with $S = 1/2$ which represents a delocalized ligand mixed valence case. Since the a_u MO transforms “ungerade” under inversion, it cannot mix with any metal d orbital. As pointed out previously, the lack of metal character in the SOMO of this *delocalized* monocation makes the spin–orbit coupling for excited states with the ground state inefficient.^{3,5} Therefore, there is little angular momentum in the presumed ground-state wave function, and the observed g shift is very small and reflects organic radical character. From the X-ray structure determination it is clear that **2** cannot have an $(a_u)^1$ ground state in the solid state since the unpaired electron is localized on one $(\text{L}^{\text{ISQ}})^{\bullet-}$ ligand whereas the other is a closed-shell quinone ${}^1\text{L}^{\text{IBQ}}$.

The fact that in the crystal structure of the monocation in **2** the excess electron is localized on one ligand, namely, the $(\text{L}^{\text{ISQ}})^{\bullet-}$ monoanionic radical, is due to the unsymmetrical ion pairing in the solid state. The presence of the intense LLCT of **2** in CH_2Cl_2 solution at 1986 nm ($\epsilon = 2.5 \times 10^4 \text{ M}^{-1} \text{ cm}^{-1}$) with its very narrow half-width at half-height of 366 cm^{-1} is more in agreement with class III¹⁴ behavior of **2** in solution.¹⁵ It is puzzling that one-electron oxidations of $[\text{M}(\text{L}^{\text{ISQ}})_2]$ ($\text{M} = \text{Ni}, \text{Pt}$), where $\text{H}_2(\text{L}^{\text{IP}})$ represents 3,5-di-*tert*-butyl-*o*-phenylenediamine and $\text{H}_2(\text{L}^{\text{IP}})$ is *N*-phenyl-*o*-phenylenediamine, yields diamagnetic dimers $\{cis\text{-}[\text{Ni}^{\text{II}}(\text{L}^{\text{ISQ}})(\text{L}^{\text{IBQ}})]_2\}^{2+}$ and $\{cis/trans\text{-}[\text{Pt}(\text{L}^{\text{ISQ}})(\text{L}^{\text{IBQ}})]_2\}^{2+}$ containing weak $\text{Ni}\cdots\text{Ni}$ and $\text{Pt}\cdots\text{Pt}$ bonding interactions at 2.800(1) and 3.031(4) Å, respectively.² In these dimers the dimensions of the four organic ligands were found to be identical; they are the arithmetic mean of the two forms $(\text{L}^{\text{ISQ}})^{\bullet-}$ and L^{IBQ} . This indicates that now the one excess electron per half-dimer is delocalized over both ligands. The nature of the $\text{M}\cdots\text{M}$ interaction is rather unclear at this point. It is also of interest to note that density functional calculations on $[\text{Pt}^{\text{II}}(\text{L}^{\text{ISQ}})(\text{L}^{\text{IBQ}})]^+$ which explicitly included relativistic effects

(14) Robin, M. B.; Day, P. *Adv. Inorg. Chem. Radiochem.* **1967**, *10*, 247.

(15) (a) Creutz, C. *Prog. Inorg. Chem.* **1983**, *30*, 1. (b) Allen, G. C.; Hush, N. S. *Prog. Inorg. Chem.* **1967**, *8*, 357.

Characterization of Members of the Series [Pd^{II}(L)₂]₂ⁿ

by using the scalar ZORA method⁵ for the geometry optimizations revealed that the above cationic form shows pronounced distortion toward a quinoidal structure for both equivalent ligands. (L^{ISQ})^{•-} and L^{IBQ} represent the one- and two-electron-oxidized forms of the unsubstituted *o*-iminophenolate(2-) dianion. Again the C–N, C–O, and C–C bond distances reflect the arithmetic mean between those observed for the (L^{ISQ})^{•-} and L^{IBQ} forms. Class III behavior with an (a_u)¹ SOMO is calculated for the monocation.⁵

Acknowledgment. We thank the Fonds der Chemischen Industrie for financial support. S.K. is grateful for a stipend from the Max-Planck Society.

Supporting Information Available: X-ray crystallographic data in CIF format. This information is available free of charge via the Internet at <http://pubs.acs.org>.

IC048292I